Dendrimers as reactive modules for the synthesis of new structure-controlled, higher-complexity megamers*

Donald A. Tomalia†, Srinivas Uppuluri, Douglas R. Swanson, and Jing Li

Center for Biologic Nanotechnology, University of Michigan, 4027 Kresge Research Bldg. II, 200 Zina Pitcher Place, Ann Arbor, MI 48109, USA

Abstract: Dendrimers are macromolecular, nanoscale objects that are widely recognized as precise, mathematically defined, covalent core-shell assemblies. As such, they are composed of quantized numbers of atoms, monomers, and terminal functional groups relative to the respective shell levels (generations) surrounding their cores. Dendrimers have been referred to as molecular-level analogs of atoms. This perspective arises from their potential to function as precise macromolecular tectons (modules), suitable for the synthesis of structure-controlled complexity beyond dendrimers. We have termed this major new class of generic structures "megamers". Our group has now synthesized such "megamer complexity" in the form of both covalent and *supra*-macromolecular *dendri*-catenanes, *dendri*-macrocycles, *dendri*-clefts, and *dendri*-clusters. The covalent *dendri*-cluster subset of megamers has been coined "core-shell tecto(dendrimers)". New mathematically defined, covalent bonding rules for tecto(dendrimer) formation are consistent with sterically induced stoichiometry (SIS) predictions and have been verified experimentally.

INTRODUCTION

Dendritic architecture is perhaps one of the most pervasive topologies observed on our planet. Innumerable examples of these patterns [1] may be found in both abiotic systems (e.g., lightning patterns, snow crystals, tributary/erosion fractals), as well as in the biological world (e.g., tree branching/roots, plant/animal vasculatory systems, neurons) [2]. In biological systems, these dendritic patterns may be found at dimensional length scales measured in meters (trees), millimeters/centimeters (fungi), or microns (neurons) as illustrated in Fig. 1. The reasons for such extensive mimicry of these dendritic topologies at virtually all dimensional length scales is not entirely clear. However, one might speculate that these are evolutionary architectures that have been optimized over the past several billions years to provide structures manifesting maximum interfaces for optimum energy extraction/distribution, nutrient extraction/distribution and information storage/retrieval.

The first abiotic laboratory synthesis of such dendritic complexity did not occur until the late 1970s to early 1980s. It required a significant digression from traditional synthesis strategies with realignment to new perspectives. These new perspectives involved the integration of several major new synthesis concepts. The result was new core-shell molecular architecture, now recognized as "dendrimers". This new perspective involved the integration of (a) staged (generations) of covalently bonded structure (mass), (b) around a molecular/atomic core, using (c) iterative chemical reaction sequences to produce (d) mathematically precise amplifications of terminal functional groups and mass as a function of generation.
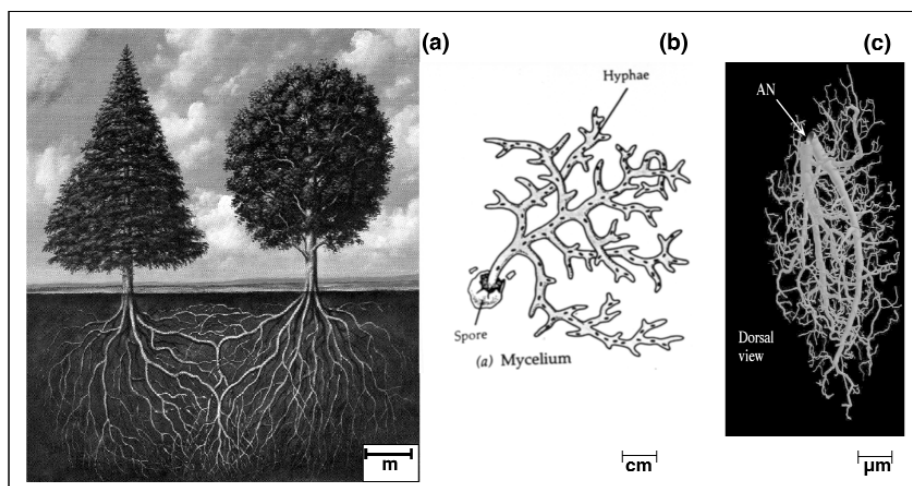
---

†Corresponding author

Fig. 1 (a) Coniferous and deciduous trees with root systems, (b) fungal anatomy, and (c) giant interneuron of a cockroach.

The nearly synchronist "cascade synthesis" by Vögtle [3] (1978) for the preparation of low-molecular-weight dendritic amines was followed closely by the macromolecular synthesis of dendrimers [4–7] (1979–1985) and arborols [8] (1985). These efforts provided routes to some of the first examples of nanoscale, dendritic architecture that extended the synthesis science of abiotic complexity well into the nanoscale region. These methods involved topological branch growth of the dendrimers from a core site or the roots of the resulting "molecular trees" and are referred to as the "divergent method". These early "divergent synthesis" strategies remain the preferred methods for commercial production of dendrimers [9].

Subsequent work by Fréchet, *et al.* [10] (1990) and Zimmerman, *et al.* [11] (1996) has provided both the "convergent and self-assembly strategies," respectively. These methods first involve synthesis of the tree branches, followed by convergent anchoring of the resulting branched assemblies ("dendrons") to the core or root of the tree. Such approaches have offered both elegant, as well as more precise structure-controlled routes to dendrimers. Using these three synthetic strategies, there are now over 100 compositionally distinct dendrimer families reported with more than 200 differentiated surface modifications. Based on unique properties, behavior and controlled nanoscale structures offered by these dendritic entities, over 3000 references have appeared in the literature within the past five years.

ORDERED COMPLEXITY IN THE ABIOTIC AND BIOTIC WORLDS

The recent seminal announcement describing complete characterization of the human genome clearly defines a new level of understanding in the area of biological complexity [12]. With this new knowledge base, the role of gene sequences in the production of both functional and structural proteins should now become comprehensible and predictable. Furthermore, the role of proteins in the determination of health or disease will become evident as we enter the next phase of biological complexity; namely, that of "proteomics"—the specific molecular-level function of all protein modules that support life.

As one reflects on evolutionary progress that defines our dimensional hierarchy of organic matter (see Fig. 2), it is apparent that it occurred in two significant phases. The first phase was "abiotic" and involved the natural molecular evolution of (I) atoms to (II) small molecules to (III) macromolecules. This began approximately 13 billion years ago, coincidentally with the "big bang" and progressed for nearly 8 to 9 billion years. The complexity reached at this point was necessary to set the stage with

(Billions of Years Ago)

"10-13   5   4.5   4   3.5   3   2.5   2   1.5   1   0.5   0

| Atoms | Small Molecules | Macro-molecules | Self Assembling Organizations | Cells | Cellular Networks (Organisms) |

I   II   III   IV   V   VI

Ordered Complexity

Abiotic Molecular Evolution

RNA   DNA

Globular Proteins, Enzymes, Hemoglobin

Viruses Antibodies Ribosomes

Bacterium   (Procaryotes) (a) E. Coli   (Eucaryotes) (a) Plants (b) Animals

Megamers

Blood Cells (Red)

Dendrimers

Multicellular Organisms

Palytoxin Bucky Balls Crown Ethers

Dendrons

Age of Microorganisms

Nucleic Acids
α-Amino Acids
CO₂, NH₃, H₂O

Branch Cells

Biotic Molecular Evolution

H, C, N, O

Monomers

Oldest Plant and Fungus Fossils

Oldest Animal Fossils

Age of Dinosaurs

Age of Mammals

Protons Neutrons Electrons

Atoms

0.1   1.0   10   100   1,000   10,000   (nm)
                              (1μ)   (10μ)   (cm m)

Dimensions

Picoscopic   Sub-Nanoscopic   Nanoscopic   Sub-Microscopic Microscopic   Macroscopic
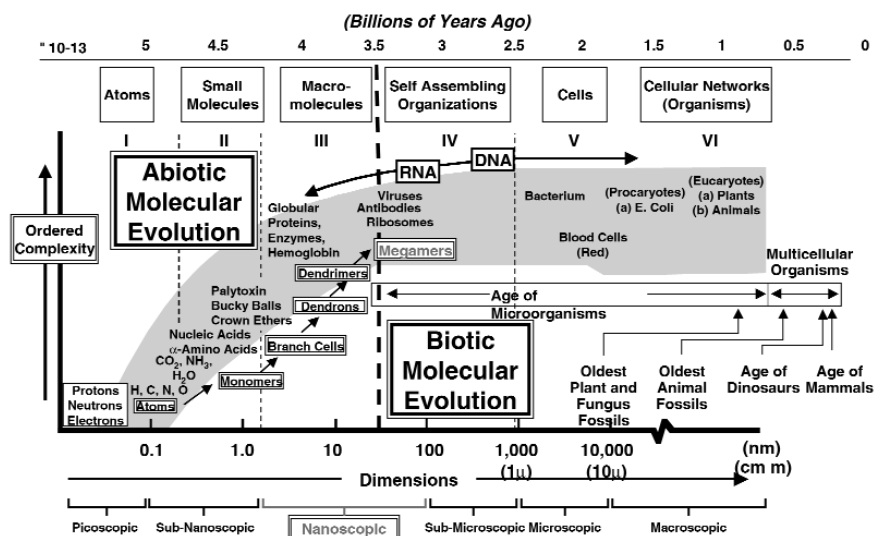
Fig. 2 Ordered complexity as a function of dimensions, evolutionary time lapse, and organic matter evolved.

appropriate building blocks for the subsequent "biotic molecular evolution". This later phase is believed to have begun approximately 3.5 billion years ago. Clearly, certain critical parameters are associated with the hierarchical ordering in each of these realms. Mass and dimensions are intuitively assumed to increase with complexity. Less obvious are the strict requirements to control critical molecular design parameters such as shape, sequencing, differentiated reactivity/association, and chemical functionality. In essence, total structural control is required at each hierarchical level for ordered complexity to progress. Beginning with the "first order" found in the minimalistic assembly of atoms from nuclei and electrons, one is able to observe certain well-defined pervasive patterns or properties which characterize each of the hierarchical levels of structural organization (I–VI) described in Fig. 2.

Advancement from one such level to the next usually involves the breaking of a property pattern characteristic for the preceding level and the establishment of a completely new order of behavior in the succeeding level. In essence, "the whole becomes not only more than, but very different from the sum of its parts" [13]. At the same time, the emerging properties for a particular dimensional, or complexity level, also provide a basis for the development of fundamental building blocks for the next higher level of complexity.

The focus of this account will be directed toward our recent efforts to attain ordered complexity beyond the dendrimer. We have coined these dendritic megamolecules or assemblies "megamers". This term is used, not only in deference to their enhanced size and intrinsic dendritic order, but also to differentiate these new ordered architectures from less ordered, classical, high-molecular-weight polymers, networks or arrays, normally synthesized by traditional statistical propagation methods.

THE DENDRITIC STATE

A comparison of traditional polymer science with dendritic macromolecular chemistry

It is appropriate to compare covalent bond formation in traditional polymer chemistry with that in dendritic macromolecular chemistry. This allows one to fully appreciate the implications/differences between the two areas in the context of structure control in concert with terminal group and mass ampli-

fication. Covalent synthesis in traditional polymer science has evolved around the use of reactive modules (AB-type monomers) that may be engaged in multiple covalent bond formation to produce large one-dimensional molecules of various lengths. Such multiple bond formation is driven either by chain reaction or poly(condensation) schemes. Staudinger first introduced this paradigm in the 1930s by demonstrating that reactive monomers could be used to produce a statistical distribution of one-dimensional molecules with very high molecular weights (i.e., $>10^6$ daltons). These covalent synthesis protocols underpin the science of traditional polymerizations. As many as 10 000 or more covalent bonds may be formed in a single chain reaction of monomers. Although megamolecules with nanoscale dimensions are often attained, relatively little control can be exercised to precisely manage critical molecular design parameters such as: sizes, atom positions, covalent connectivity (i.e., other than linear topologies), or molecular shapes [14,15]. These polymerizations usually involve AB-type monomers based on substituted ethylenes, strained small ring compounds, or AB-type monomers which may undergo polycondensation reactions. Such chain propagation reactions may be initiated by free radical, anionic, or cationic initiators. Multiple covalent bonds are formed per chain sequence, wherein the average lengths are determined by monomer to initiator ratios. Generally, polydispersed structures are obtained that are statistically controlled. All three classical polymer architectures; namely, Class I— linear, Class II—cross-linked (bridged), and Class III—branched topologies are routinely prepared by these methods (Fig. 6) [16–18].

In the case of dendron/dendrimer syntheses, one may view those processes as simply sequentially staged (generations), quantized polymerization events. The assembly of reactive monomers [19], branch cells [20,21], or dendrons [11] around atomic or molecular cores to produce dendrimers according to divergent/convergent dendritic branching principles has been well demonstrated [22]. Such systematic filling of space around cores with branch cells, as a function of generational growth stages (branch cell shells), to give discrete, quantized bundles of mass has been shown to be mathematically predictable [23]. Predicted theoretical molecular weights have been confirmed by mass spectroscopy [24–26] and other analytical methods [27]. In all cases, their growth and amplification is driven by the following general mathematical expressions (Fig. 3).
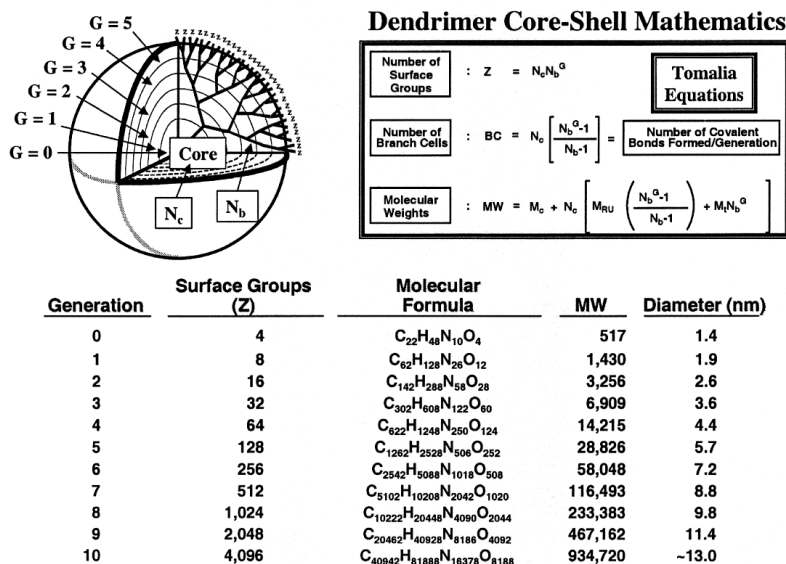

Dendrimer Core-Shell Mathematics

Number of Surface Groups: $Z = N_c N_b^G$

Number of Branch Cells: $BC = N_c \left[\dfrac{N_b^G - 1}{N_b - 1} \right]$ = Number of Covalent Bonds Formed/Generation

Molecular Weights: $MW = M_c + N_c \left[M_{RU} \left(\dfrac{N_b^G - 1}{N_b - 1} \right) + M_t N_b^G \right]$

Tomalia Equations

Generation	Surface Groups (Z)	Molecular Formula	MW	Diameter (nm)
0	4	$C_{22}H_{48}N_{10}O_4$	517	1.4
1	8	$C_{62}H_{128}N_{26}O_{12}$	1,430	1.9
2	16	$C_{142}H_{288}N_{58}O_{28}$	3,256	2.6
3	32	$C_{302}H_{608}N_{122}O_{60}$	6,909	3.6
4	64	$C_{622}H_{1248}N_{250}O_{124}$	14,215	4.4
5	128	$C_{1262}H_{2528}N_{506}O_{252}$	28,826	5.7
6	256	$C_{2542}H_{5088}N_{1018}O_{508}$	58,048	7.2
7	512	$C_{5102}H_{10208}N_{2042}O_{1020}$	116,493	8.8
8	1,024	$C_{10222}H_{20448}N_{4090}O_{2044}$	233,383	9.8
9	2,048	$C_{20462}H_{40928}N_{8186}O_{4092}$	467,162	11.4
10	4,096	$C_{40942}H_{81888}N_{16378}O_{8188}$	934,720	~13.0

Fig. 3 (a) Dendrimer propagation mathematics; where: N_c, N_b = core, branch cell multiplicities; respectively, and G = generation; (b) mathematically defined values for surface groups (Z), molecular formulae and molecular weights (MW) as a function of generation for the (ethylenediamine core), poly(amidoamine) (PAMAM) dendrimer family.

Mathematically, the number of covalent bonds formed per generation (reaction step) in a dendron/dendrimer synthesis varies as a power function of the reaction steps (Fig. 4) [28]. This analysis shows that covalent bond amplification occurs in all dendritic strategies. This feature clearly differentiates dendritic processes from covalent bond synthesis found in traditional organic chemistry or polymer chemistry. Polymerization of AB_2 or AB_x monomers leading to random, hyperbranched polymers also adhere approximately to these mathematics, however, in a more statistical fashion.

In addition to the extraordinary structure control observed for dendrimers, perhaps the next most outstanding feature is their mimicry of globular proteins. Based on their systematic, dimensional length scaling (Fig. 4) and electrophoretic behavior, (Fig. 5) they are often referred to as "artificial proteins". These fundamental properties have in fact led to their commercial use as globular protein replacements for gene expression (therapy) [29,30] and immunodiagnostics. [31–33].
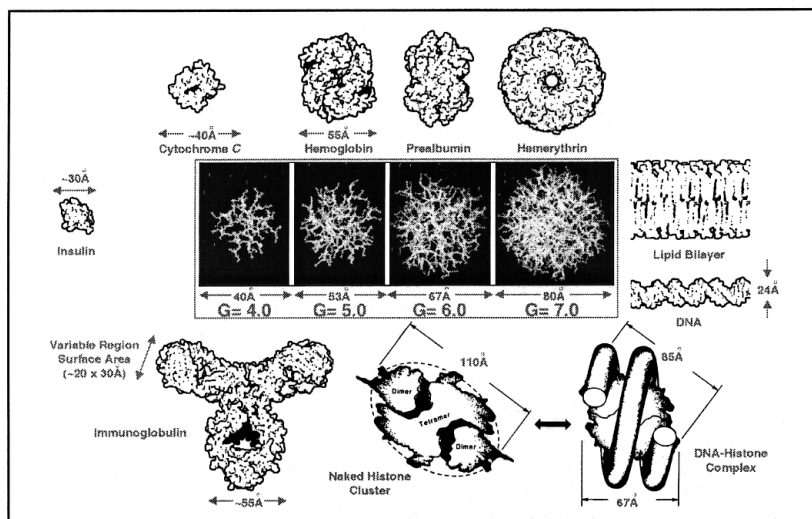
Fig. 4 A dimensionally scaled comparison of a series of poly(amidoamine) (PAMAM) dendrimers (NH_3 core; G = 4–7) with a variety of proteins, a typical lipid bilayer membrane, and DNA.
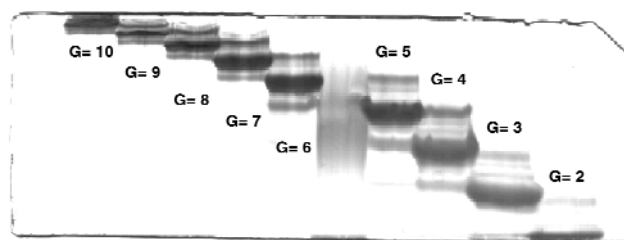
Fig. 5 Electrophoretogram of a series of poly(amidoamine) (PAMAM) dendrimers (ethylenediamine core; G = 2–10) analyzed on a 5–40% T polyacrylamide gel. A 0.1 M citric acid buffer, pH 3.0 was used as the run buffer in both the upper and lower tanks. The unlabeled smear in the middle of the gel is a proprietary sample. The middle band in each lane corresponds to the mono-dendrimers as a function of generation (G). The slowest bands in each dendrimer lane are dimers of that generation which may be compared to (G-1) bands, which migrate the fastest in each lane.

Dendritic architecture has been widely recognized as a fourth major class of macromolecular architecture [16–18]. The signature for such a distinction is the unique repertoire of new properties manifested by this class of polymers [9,34–36]. This architectural class consists of three dendritic sub-classes; namely: (IVa) random hyperbranched polymers, (IVb) dendrigrafts, and (IVc) dendrimers (Fig. 6). This subset order (Iva–c) describes the relative degree of structural control present in each of these dendritic architectures. New properties and applications for these dendritic polymer subsets have been reviewed elsewhere [9,21]. Within the realm of traditional macromolecular structure, random hyper-branched polymers (IVa) may be viewed as penultimate precursors residing between thermoplastic architectures (i.e., linear (I)/branched (III)) structures and thermoset architectures as illustrated in Fig. 6 [37]). As such, the dendritic state may be visualized as an advancement from a lower order (i.e., Class I-III) to a somewhat higher level of structural complexity [38,39]. Recent developments now demonstrate that these transitions involve various levels of structural control. It is widely recognized that in contrast to random hyperbranched polymers, the subsets dendrigrafts and dendrimers represent a unique combination of high complexity with extraordinary structure control. As such, covalent bridging or cross-linking of these modules has proven to give rise to a completely new class (V) of more ordered complexity which we have coined—"megamers".

MEGAMERS

In our very first dendrimer paper, we proposed "dendrimers as fundamental building blocks to a new class of topological macromolecules which we referred to as 'starburst' polymers" [40]. Quite remarkably in the 15 years that have lapsed, over 3000 references have appeared in the literature related to dendrimers and dendritic polymers with barely a handful of references focused on the above concept [39]. Clearly, the area of megamer synthesis and characterization is presently in its infancy. Meanwhile, since the term "starburst"' has been adopted by the commercial world as a registered trademark-Starburst® (The Dow Chemical Company has purchased all dendritic polymer related intellectual property from
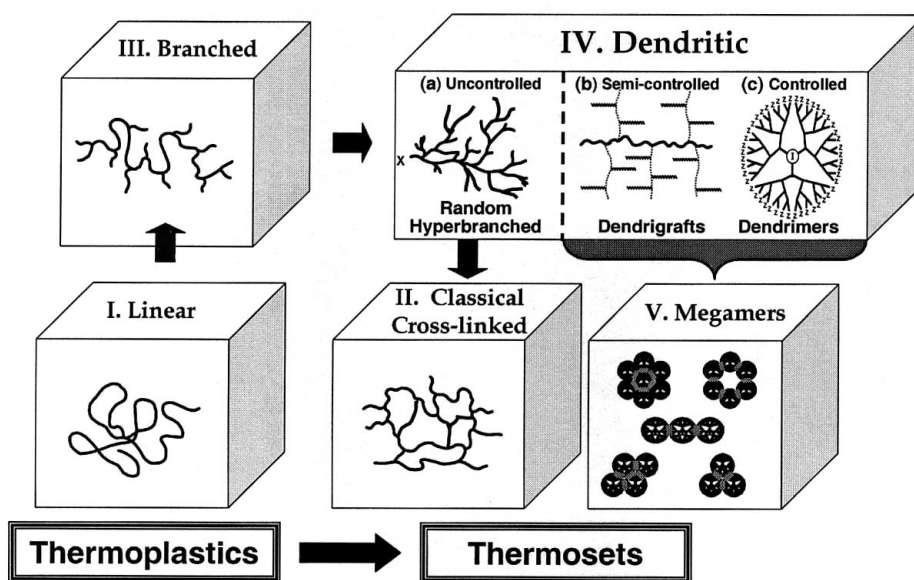

Fig. 6 Major macromolecular architectures (I–V). Dendritic architecture (IV) may be categorized into statistical (uncontrolled) and controlled subsets as illustrated.

Dendritech, Inc., Midland, USA), we propose the generic term "megamers" to describe these new architectures. In this account, we present a brief overview of our recent work, which includes the general areas of **Statistical Megamer Constructions** and **Structure-Controlled Megamer Constructions.**

STATISTICAL MEGAMERIC CONSTRUCTIONS

Statistical self-assembling three-dimensional megamers

In our earliest work [40], it was apparent that amine-terminated poly(amidoamine) (PAMAM) dendrimers exhibited a great propensity to form self-assembling megameric clusters. Efforts to obtain transmission electron micrographs (TEM) of individual dendrimers were invariably accompanied by a background of cluster formation even at high dilutions.

This property has subsequently been well documented by Amis *et al.* [41] using cryo-TEM techniques. Using G = 10, amine-terminated PAMAM dendrimers, these investigators noted large, ordered spheroidal clusters with diameters of approximately 17 dendrimers wide ($\cong$29 nm) at high solution concentration and smaller clusters of about 3–8 dendrimers wide at lower concentrations.

Self-assembled, three-dimensional dendritic network structures possessing critical π-type surface groups have been reported to exhibit unique electrical conducting properties. Miller/Tomalia and coworkers [42] observed unusually high conductivities (i.e., 18 s/cm at 90% humidity) for generation = 3 PAMAM dendrimers surface modified with cationically substituted naphthalene diimides. In all cases, the conductivity was electronic and isotropic. Near infrared spectra showed the formation of extensive π-stacking, which presumably favored electron hopping *via* a three-dimensional network.

More recent work by Aida *et al.* [43] reported the electrostatically directed assembly of porphyrin core dendrimers to produce large infinite network aggregates. Energy transfer constants were obtained and used to determine distances between acceptors and donors; thus, demonstrating that communication occurred within these domains.

Statistical self-assembling two-dimensional megamers

Poly(amidoamine) dendrimers (G = 9, EDA core) readily form two-dimensional, self assembled, megameric packing arrays on freshly cleaved mica surface as seen in Figs. 7–8. This top-view AFM image reveals well-ordered particle packing except for some vacancies, dislocations, and grain bound-
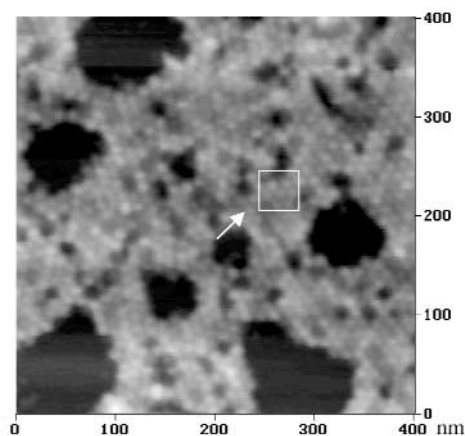

Fig. 7 Tapping mode AFM image of G9 PAMAM dendrimer molecules on mica surface. Sample prepared by placing 6 µl of a dilute aqueous solution, conc. 5×10^{-3} % (w/w) G = 9 on a freshly cleaved mica surface and allowing the film to dry slowly at room temperature.

aries. Most areas show very dense packing of globular G = 9 dendrimer, exhibiting an obvious hexagonal order as indicated within the square of Fig. 7. The size of these densely packed G = 9 dendrimer molecules by AFM measurement is approximately 12.8 nm in diameter. This suggests that dense packing of G = 9 dendrimer molecules reduce the deformation, which normally occurs with single G = 9 dendrimers on a mica surface.

It was also found that the megameric deposition pattern changes dramatically if the amount of G = 9 solution placed on the mica surface is decreased from 6 µl to 3 µl as illustrated in Fig. 8. It can be seen that the dendrimers assembled to form an inter-linked chain texture. Some hexagonal pattern can be observed within these arrays as indicated in Fig. 8. However, very few isolated single G = 9 dendrimer molecules were found even after multiple scans of several areas. These results suggest that both the chemical and physical characteristics of the G = 9 PAMAM dendrimers strongly influence its interfacial behavior to produce the observed particle pattern. Important features such as its high surface functional group density, in combination with the propensity of amines to express significant neighboring group hydrogen bonding effects, undoubtedly impact its relative rigidity and robust spherical shape compared to earlier generations.

Figure 9 shows a very striking perturbation of the G = 9 PAMAM self assembly that is possible by applying a nitrogen gas stream flowing at approximately a 35° angle to the sample surface, after
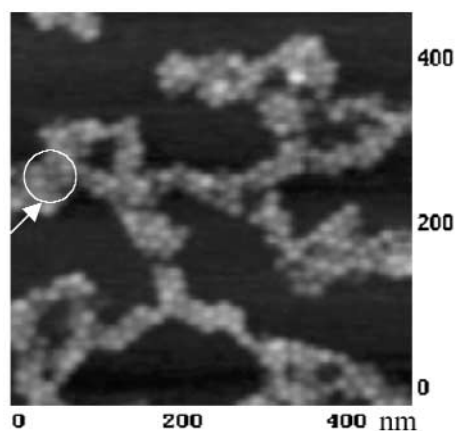

Fig. 8 Tapping mode AFM image of G9 dendrimers on mica surface. Sample prepared under the same conditions as in Fig. 1, except that 3 µl solution was placed onto the freshly cleaved mica surface.
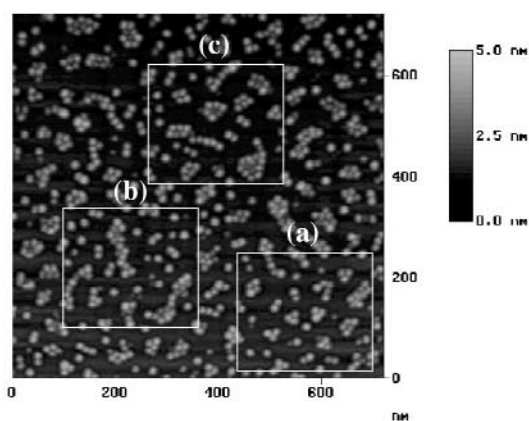

Fig. 9 Tapping mode AFM images of G9 PAMAM dendrimer molecules on mica surface. Sample prepared under the same conditions as in Figure 8, except for the addition of drying by a nitrogen stream.

placing 3 µl of G = 9 solution on a freshly cleaved mica surface at room temperature. A vast assortment of small domain self-assembly patterns are observed. One might view this as a megameric, self-assembly library for G = 9 PAMAM dendrimers under these conditions. Figure 10 exhibits single isolated G9 dendrimer molecules, dimers, trimers, and other more complex packing patterns. These megameric patterns may be seen more clearly in the high magnification images shown in Figs. 10a–c. A single G = 9 dendrimer molecule is enclosed by a circle, whereas a dimer is identified with an oval and the trimer by the square in Fig. 10a.

Application of small nitrogen gas flow forces, not only caused partitioning of the large megameric arrays (Fig. 8) into small discrete domains (Figs. 9a–c), but also induced changes in the shape and size of the G = 9 dendrimer. Some of the G = 9 molecules have the appearance of having been squeezed together, their shape contorted into irregular, unsymmetrical forms instead of their characteristic spheroidal shapes, indicated by arrows 1 and 2 in image (Fig. 10b). These results suggest that dendrimers are soft, spongy, and elastic. It appears their shapes may be somewhat distorted by their participation in these small self-assembled domains. A large variety of self-assembly architectures are observed. Some resemble curved linear catenations as in Fig. 10c (arrow 3); whereas, other assemblies such as barbell-type dimers, pyramidal trimers, parallelogram-type tetramers, and hexamers are noted.

Statistical three-dimensional covalent megamers

In our very earliest work [40], covalent dendrimer bridging was often noted when amine-terminated PAMAM dendrimers (i.e., G = 1–10) were heated to higher temperatures (i.e., >175–200 °C). Under these conditions, gelation was observed and believed to be due to transamidation reactions, accompanied by the loss of ethylenediamine.

Subsequent work by Tomalia *et al.* [39] reported a more convenient method for producing statistical covalent, three-dimensional megamers. Combining equimolar amounts of a nucleophile-terminated (i.e., –NH_2) dendrimer with an electrophile-terminated (i.e., –CO_2Me) dendrimer produced statistical megamers which were fractionated and examined by TEM.

Heating stoichiometric amounts of G = 4.5 (–CO_2Me) terminated PAMAM dendrimer with G = 5.0 (–NH_2) terminated dendrimer gives a gel with a maximum ester to amide conversion of approximately 30% after 24 h at 125 °C. The partially insoluble gel was extracted with methanol and examined as a post-gelation solution phase by electron microscopy. Using osmium tetraoxide staining tech-
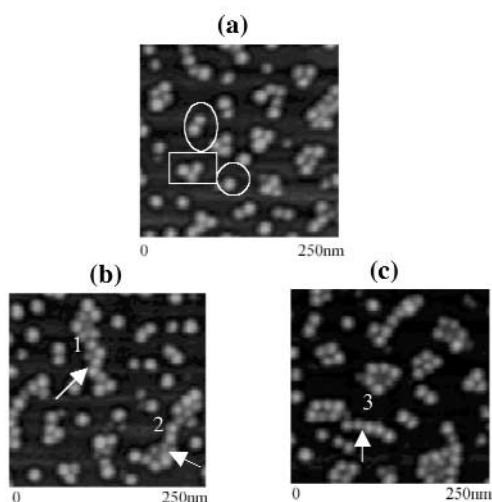

Fig. 10 Magnified images from Fig. 9.

niques, the electron micrograph revealed a population of covalent megameric clusters that have cross-sectional dimensions ranging from ≅16–80 nm in diameter. Figure 11 shows an electron micrograph of a larger cluster that is approximately 50 × 60 nm in diameter. Most remarkable, however, are the extraordinary topological features that may be characterized as *dendri*-macrocycles, *dendri*-catenanes or *dendri*-clefts. The cavities produced by the unique packing orders derived from the dendrimer dimensions (i.e., 5 × 10 nm) differ dramatically from those observed for cyclodextrins (i.e., 0.6–1.2 nm). This suggests novel opportunities for catalysis or size-selective adsorption applications.

STRUCTURE-CONTROLLED MEGAMER CONSTRUCTIONS

Core-shell tecto(dendrimers): A subclass of megamers

Core-shell architecture is a very recognizable concept in the lexicon of science. Beginning with the first observations by Galileo concerning the heliocentricity of the solar system [44], progressing to the planetary model first proposed by Rutherford [45] and expounded upon by Bohr [46], such architecture has been broadly used to describe the influence that a central focal point component may exercise on its surrounding satellite components.

Such has been the case recently at the subnanoscale level. Rebek *et al.* have described [47] the influence that a guest-molecule may have on self-assembling components that are directed by hydrogen-bonding preferences and the filling of molecular space. It was shown that hydrogen-bonding preferences combined with spacial information such as molecular curvature may be used to self-assemble a single core-shell structure at the subnanoscopic scale level (i.e., <1 nm).

At the nanoscale dimensional level it was shown by Hirsch *et al.* [48] that C_{60}-fullerenes could be used as a core tecton to construct a core-shell molecule with T_b-symmetrical C_{60} core and an extraordinarily high branching multiplicity of 12.

As described earlier, the assembly of reactive monomer [19] branch cells [20,21] around atomic or molecular cores to produce dendrimers according to divergent/convergent dendritic branching principles is well demonstrated [22]. Recent studies have shown that poly(amidoamine) PAMAM den-
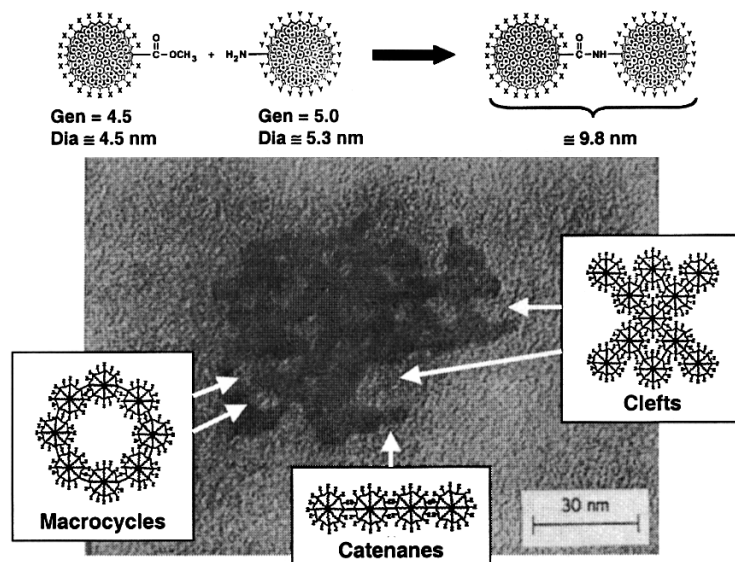

Fig. 11 TEM of osmium tetraoxide stained clusters presented on a grid. This sample was obtained from the high-molecular-weight fraction of methanol soluble decantate.

drimers are indeed very well-defined, systematically sized spheroids [41] as a function of generation level. Furthermore, evidence has been obtained by SANS studies to shown that these PAMAM dendrimers behave as originally described by de Gennes [49]. The terminal groups remain largely at the periphery and are presented *exo* with virtually no backfolding [50,51].

These dendritic synthetic strategies have allowed the systematic control of molecular structure as a function of size [41], shape [52], and surface/interior functionality [34]. Such synthetic strategies have allowed construction of dendrimeric structures with dimensions that extend well into the lower nanoscale regions (i.e., 1–30 nm). It is now time to consider the possibilities of using dendrimers as fundamental modules for the synthesis of structure-controlled complexity beyond the individual dendrimer.

Anticipating the use of these nanoscale modules in a variety of construction operations, we examined the random parking of spheres upon spheres [53]. From this study, it was both surprising and pleasing to find that at low values of radii ratios (i.e., <1.2), absolutely beautiful, symmetrical properties appeared as illustrated in Fig. 12a. However, at higher radii ratios, the mathematics resolved into the following Mansfield–Tomalia–Rakesh general expression. From this relationship, it is possible to calculate the number of spheroidal dendrimers one would expect to place in a shell around a core dendrimer as a function of their respective radii (see Figs. 12b–c).

Inspired by these derived values for shell filling around a "central dendrimer core", we devised several synthetic approaches to test this hypothesis. The first method involved the direct covalent reaction of a nucleophilic dendrimer core with an excess of an electrophilic dendrimer shell reagent. This strategy produced semi-controlled megamer structures and is referred to as the (a) Direct Covalent Bond Formation Method. The second method involved self-assembly by electrostatic neutralization of a cationic dendrimer core with excess anionic shell reagent to give the (b) Self Assembly with Subsequent Covalent Bond Formation Method. In each case, relatively mono-dispersed products are obtained. We call these new megameric architectures "core-shell (tecto)dendrimers".
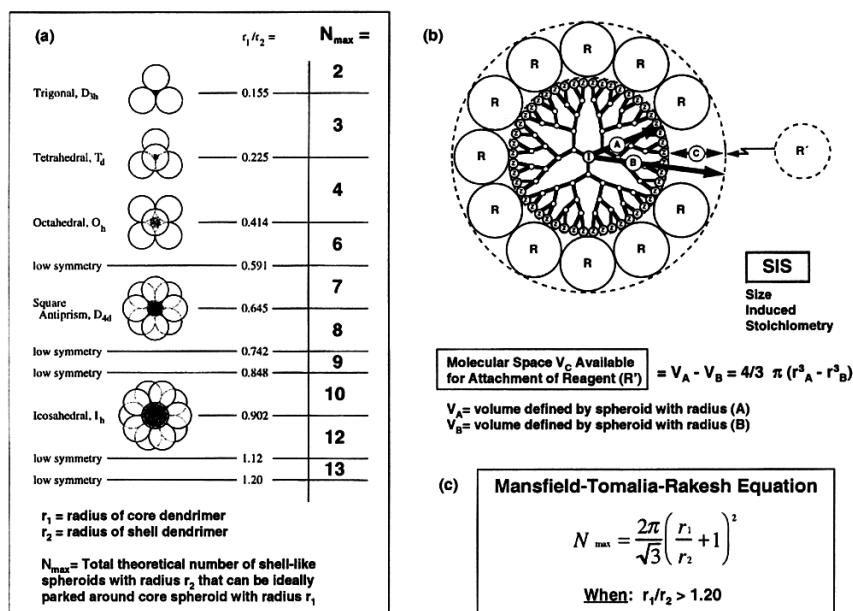

Fig. 12 (a) Symmetrical properties for core-shell structures where $r_1/r_2 < 1.20$. (b) Sterically induced stoichiometry (SIS) based on respective radii (r_1) and (r_2) core and shell dendrimers, respectively. (c) Mansfield–Tomalia–Rakesh equation for calculation of maximum shell filling when $r_1/r_2 > 1.20$.

SEMI-CONTROLLED MEGAMERIC ASSEMBLIES

Direct covalent bond formation method—partially filled shell model

This route produces partially filled shell structures and involves the reaction of a nucleophilic dendrimer core reagent with an excess of electrophilic dendrimer shell reagent as illustrated in Fig. 13 [38,54].

Various poly(amidoamine) PAMAM dendrimer core reagents (i.e., either amine or ester functionalized) were allowed to react with an excess of appropriate PAMAM dendrimer shell reagents. The reactions were performed at 40 °C in methanol and monitored by FTIR, ^{13}C-NMR, size-exclusion chromatography (SEC) and gel electrophoresis. Conversions in step (a) were followed by the formation of higher molecular weight, shorter retention time products using SEC. Additional evidence was gained by observing loss of the migratory band associated with the dendrimer core reagent present in the initial reaction mixture, accompanied by the formation of a higher molecular weight product, which displayed a much shorter migratory band position on the electrophoretic gel. In fact, the molecular weights of the resulting core-shell tecto(dendrimer) could be estimated by comparing the migratory time of the core-shell product (PAGE results, Table 1) with the migration distances of the PAMAM dendrimers (e.g., G = 2–10) used for their construction [27] (Fig. 5).

It was important to perform capping reactions on the surface of the resulting ester terminated core-shell products in order to pacify the highly reactive surfaces against further reaction. Preferred capping reagents were either 2-amino-ethanol or *tris*-hydroxymethyl aminomethane. The capping reaction, step (b), was monitored by following the disappearance of an ester band at 1734 cm^{-1}, using FTIR. Isolation and characterization of these products proved that they were indeed relatively mono(dispersed) spheroids as illustrated by atomic force microscopy (AFM). It was very important to perform the AFM analysis at very high dilution to avoid undesirable core-shell molecular clustering. In spite of these efforts, a small amount of clustering is still observed.

A distinct core-shell dimensional enhancement was observed as a function of the sum of the core-shell generation values used in the construction of the series (e.g., core shell: G4/G3, <G5/G3, <G6/G4, and <G7/G5). This is in sharp contrast to nondescript polydispersed dendrimer cluster/gel formation observed for 1:1 reaction ratios described in our earlier work [39] in this report (Fig. 11).

Molecular weights for the final products were determined by MALDI-TOF-MS or (polyacrylamide) gel electrophoresis (PAGE). They were corroborated by calculated values from AFM dimension data (Table 1) and were found to be in relatively good agreement within this series (Table 1).

Calculations based on these experimentally determined molecular weights allowed the estimation of shell filling levels for respective core-shell structures within this series. A comparison with mathe-
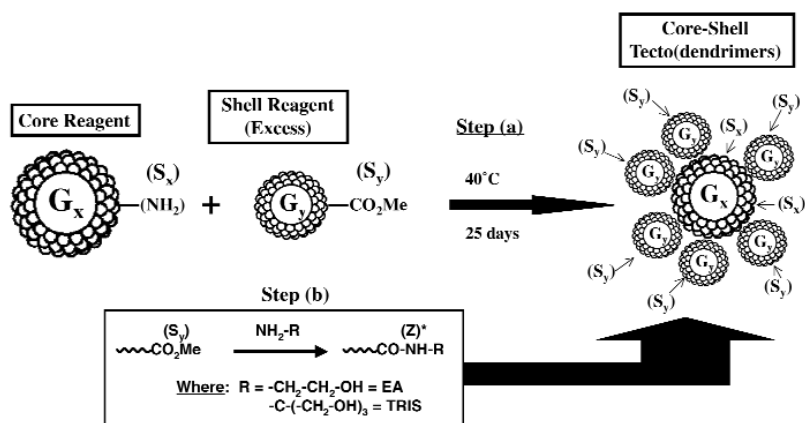

Fig. 13 Reaction scheme for partial shell-filled model, step (a); step (b) describes surface capping reactions.

matically predicted saturated shell structure values reported earlier [53], indicates these core-shell structures are only partially filled (i.e., 40–66% of fully saturated values, see Table 1).

Functional group differentiated clefts are produced on the surfaces of these unique, partially filled tecto(dendrimer) core-shell structures. This suggests rich possibilities for catalytic sites and other novel surface modifications that are presently under examination in our laboratory.

CONTROLLED MEGAMERIC ASSEMBLIES

Self-assembly with subsequent covalent bond formation method—saturated shell model

The chemistry used in this approach involved the combination of an amine terminated core dendrimer with an excess of carboxylic acid-terminated, shell reagent dendrimer (Fig. 14) [55]. These two charge

Table 1

$X;[(Y)(Z^*)]_n$	$G4[(G3); (EA)]_n$	$G5(G3); (TRIS)]_n$	$G6(G4); (TRIS)_n$	$G7(G5); (TRIS)_n$
Theoretical shell saturation levels(n)	9	15	15	15
Observed shell saturation levels (n*)	4	8–10	6–8	6
% Theoretical shell saturation levels	44%	53–66%	40–53%	40%
MALDI-TOF-MS (MW)	56 496	120 026	227 606	288 970
PAGE (MW)	58 000	116 000	233 000	467 000
AFM: observed dimensions	25×0.38 nm	33×0.53 nm	38×0.63 nm	43×1.1 nm
CALC (MW)	(D,H) 56 000	(D,H) 136 000	(D,H) 214 000	(D,H) 479 000

*Where: X = dendrimer core reagent; generation Y = dendrimer shell reagent, and Z = surface group functionality.
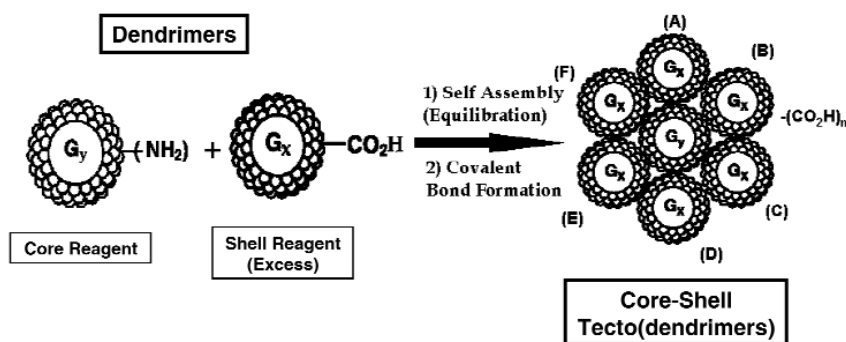

Fig. 14 Reaction scheme for saturated shell model. Where: (A–E) are –(CO$_2$H) terminated.

Table 2

Core-shell compound	**1**	**2**	**3**	**4**
Formula: [G"X"A]/{G"Y"C}$_n$[a]	[G5A]/{G3C}$_n$	[G6A]/{G3C}$_n$	[G7A]/{G3C}$_n$	[G7A]/{G5C}$_\underline{n}$
MW (calculated)[b]	137 350	197 700	301 270	537 300
Number of shell tectons, observed[c]/theoretical[d]:	10/12	13/15	15/19	9/12
ratio	0.83	0.87	0.79	0.75
MALDI–MS (MW)	114 000	172 000	238 000	403 000
PAGE (MW)	120 000	168 000	250 000	670 000
AFM: diameter (nm)	—	23.5 ± 6.7	28.2 ± 4.5	28.0 ± 4.2
height (nm)	—	2.15 ± 0.5	2.64 ± 0.8	3.84 ± 1.0
estimated MW[e]	—	195 000	369 000	469 000

[a]In the notation [G"X"A]/{G"Y"C}$_\underline{n}$ above, $\underline{n}$ = number of dendrimer shell molecules {G"Y"C} surrounding the dendrimer core molecule [G"X"A], where: [G"X"A] represents amine-terminated, EDA core, generation "X", PAMAM dendrimer core reagent, and [G"X"C] represents carboxylic acid-terminated, EDA core, generation "X" PAMAM dendrimer core reagent, and [G"Y"C] represents carboxylic acid-terminated, EDA core, generation "Y", PAMAM dendrimer shell reagent.
[b]MW of theoretical number of shell dendrimer tectons plus core tecton, as [53] determined from MALDI-MS data for individual core and shell tecton molecular weights. Values used for *n* in these calculations were obtained by using the Mansfield–Tomalia–Rakesh equation described.
[c]Based on the experimental MALDI-MS molecular weights of the tecto(dendrimer)s as isolated.
[d]The theoretical number (*n*) of dendrimer shell molecules that would be expected to surround a specific dendrimer core molecule according to the Mansfield–Tomalia–Rakesh equation [53].
[e]See reference [56].

differentiated species were then allowed to equilibrate and self-assemble into the electrostatically driven core-shell tecto(dendrimer) architecture, followed by covalent fixing of these charge neutralized dendrimer contacts with carbodiimide reagents. Reactions were readily monitored by SEC, gel electrophoresis, AFM, and MALDI-TOF mass spectroscopy. As might be expected, data show that the self-assembly method provides for more efficient parking of the dendrimer shell reagents around the dendrimer core to yield very high saturation levels (i.e., 75–83%) as shown in Table 2. Our present experimentation indicates that this method will allow the assembly of additional shells in a very systematic fashion to produce precise nanostructures that transcend the entire nanoscale region (1–100 nm).

CONCLUSIONS

"Molecular complexity can be used as an indicator of the frontiers of synthesis since it often causes failures which expose gaps in existing methodology. The realization of such limitations can stimulate the discovery of new chemistry and new ways of thinking about synthesis."

—E. J. Corey

Presently, society is seeking understanding at new levels of molecular complexity encompassed by two important emerging scientific fields; namely, nanotechnology and proteomics. Therefore, it is time to examine our skills and options for performing abiotic synthesis and "bottom-up constructions" in these size domains. In view of the remarkable "protein mimicry" offered by dendrimers, as well as the demonstrated use of dendrimers as reactive modules to produce higher-ordered nanoscale structures, such as megamers, it is appropriate to be optimistic about our quest for ordered abiotic "complexity beyond the individual dendrimer".

ACKNOWLEDGMENTS

REFERENCES

1. D. Thompson. *On Growth and Form*, Cambridge University Press, London (1987).
2. A. Mizrahi, E. Ben-Ner, M. J. Katz, K. Kedem, J. G. Glusman, F. Libersat. *J. Comp. Neurol.* **422**, 415 (2000).
3. E. Buhleier, W. Wehner, F. Vögtle. *Synthesis* 155 (1978).
4. D. A. Tomalia. In *Flory-Pauling Macromolecular Conference: Frontiers in Synthetic Polymer Chemistry*, Santa Barbara, CA, January 1983.
5. D. A. Tomalia, J. R. Dewald, M. J. Hall, S. J. Martin, P. B. Smith. In *Preprints of the 1st SPSJ Int. Polym. Conf., Society of Polymer Science*, p. 65, Kyoto, Japan, August 1984.
6. D. A. Tomalia. In *Akron Polymer Lecture Series*, Akron, OH, April 1984.
7. D. A. Tomalia. In *ACS Great Lakes/Central Regional Meeting*, Kalamazoo, MI, May 1984.
8. G. R. Newkome, Z.-Q. Yao, G. R. Baker, V. K. Gupta. *J. Org. Chem.* **50**, 2003 (1985).
9. D. A. Tomalia and R. Esfand. *Chem. Ind.* **11**, 416 (1997).
10. C. J. Hawker and J. M. J. Fréchet. *J. Am. Chem. Soc.* **112**, 7638 (1990).
11. F. Zeng and S. C. Zimmerman. *Chem. Rev.* **97**, 1681 (1997).
12. N. Wade. *The New York Times,* "Genetic Code of Human Life is Cracked by Scientists", June 27, 2000, Section D.
13. P. W. Anderson. *Science* **177**, 393 (1972).
14. K. Matyjaszewski. *ACS Symposium Series 685,* American Chemical Society, Washington DC (1997).
15. K. Matyjaszewski. *Cationic Polymerizations: Principles and Practical Applications*, p. 1. Marcel Dekker, New York, 1996.
16. D. A. Tomalia. *Macromol. Symp.* **101**, 243 (1996).
17. A. K. Naj. *The Wall Street Journal*, "Persistent Inventor Markets a Molecule", February 26, 1996, B1.
18. P. R. Dvornic and D. A. Tomalia. *Science Spectra* **5**, 36 (1996).
19. D. A. Tomalia. *Sci. Am.* **272**, 62 (1995).
20. G. R. Newkome, C. N. Moorfield, F. Vögtle. *Dendritic Molecules*, VCH, Weinheim, (1996).
21. J. M. J. Fréchet. *Science* **263**, 1710 (1994).
22. O. A. Matthews, A. N. Shipway, J. F. Stoddard. *Prog. Polym. Sci.* **23**, 1 (1998).
23. D. A. Tomalia. *Adv. Mater.* **6**, 529 (1994).
24. G. J. Kallos, D. A. Tomalia, D. M. Hedstrand, S. Lewis, J. Zhou. *Rapid Commun. Mass Spectrom.* **5**, 383 (1991).
25. P. R. Dvornic and D. A. Tomalia. *Macromol. Symp.* **98**, 403 (1995).
26. J. C. Hummelen, J. L. J. van Dongen, E. W. Meijer. *Chem. Eur. J.* **3**, 1489 (1997).
27. H. M. Brothers II, L. T. Piehler, D. A. Tomalia. *J. Chromatogr. A* **814**, 233 (1998).
28. M. K. Lothian-Tomalia, D. M. Hedstrand, D. A. Tomalia. *Tetrahedron* **53**, 15495 (1997).
29. J. F. Kukowska-Latallo, A. U. Bielinska, J. Johnson, R. Spindler, D. A. Tomalia, J. R. Baker Jr. *Proc. Natl. Acad. Sci. USA* **93**, 4897 (1996).
30. J. D. Eichman, A. U. Bielinska, J. F. Kukowska-Latallo, J. R. Baker Jr. *Pharm. Sci. & Tech. Today* **3** (7), 232 (2000).

31. P. Singh, F. Moll III, S. H. Lin, C. Ferzli, K. S. Yu, K. Koski, R. G. Saul. *Clin. Chem.* **40** (9), 1845 (1994).
32. P. Singh, F. Moll III, S. H. Lin, C. Ferzli. *Clin. Chem.* **42** (9), 1567 (1996).
33. P. Singh. *Bioconjugate Chem.* **9**, 54 (1998).
34. D. A. Tomalia, A. M. Naylor, W. A. Goddard III. *Angew. Chem. Int. Ed. Engl.* **29**, 138 (1990).
35. J. M. J. Frèchet, C. J. Hawker, I. Gitsov, J. W. Leon. *J. M.S.-Pure Appl. Chem.* **A33 (10)**, 1399 (1996).
36. F. Vögtle and M. Fischer. *Angew. Chem. Int. Ed.* **38**, 884 (1999).
37. K. Dusek. *TRIP* **5** (8), 268 (1997).
38. S. Uppuluri, D. R. Swanson, H. M. Brothers II, L. T. Piehler, J. Li, D. J. Meier, G. L. Hagnauer, D. A. Tomalia. *Polym. Mater. Sci. & Eng.* (*ACS*) **80**, 55 (1999).
39. D. A. Tomalia, D. M. Hedstrand, L. R. Wilson. In *Encylopedia of Polymer Science and Engineering*, Vol. Index Volume, 2nd ed., p. 46. Wiley, New York (1990).
40. D. A. Tomalia, H. Baker, J. Dewald, M. Hall, G. Kallos, S. Martin, J. Roeck, J. Ryder, P. Smith. *Polym. J.* (*Tokyo*) **17**, 117 (1985).
41. J. L. Jackson, H. D. Chanzy, F. P. Booy, B. J. Drake, D. A. Tomalia, B. J. Bauer, E. J. Amis. *Macromolecules* **31**, 6259 (1998).
42. L. L. Miller, R. G. Duan, D. C. Tully, D. A. Tomalia. *J. Am. Chem. Soc.* **119**, 1005 (1997).
43. N. Tomioka, D. Takasu, T. Takahashi, T. Aida. *Angew. Chem. Int. Ed.* **37(11)**, 1531 (1998).
44. G. Galileo. *Dialogue Concerning the Two Chief World Systems: Ptolemaic and Copernican*, University of California Press, Berkeley (1967).
45. B. Pullman. *The Atom in the History of Human Thought*, University Press, New York (1998).
46. N. Bohr. *Nobel Laureate Lecture* (1922).
47. T. Martin, U. Obst, J. Rebek Jr. *Science* **281**, 1842 (1998).
48. X. Camps, H. Schonberger, A. Hirsch. *Chem. Eur. J.* **3** (4), 561 (1997).
49. P. G. de Gennes and H. J. Hervet. *J. Physique-Lett. (Paris)* **44**, 351 (1983).
50. A. Topp, B. J. Bauer, D. A. Tomalia, E. J. Amis. *Macromolecules* **32**, 7232 (1999).
51. A. Topp, B. J. Bauer, J. W. Klimash, R. Spindler, D. A. Tomalia. *Macromolecules* **32**, 7226 (1999).
52. R. Yin and D. A. Tomalia. *J. Am. Chem. Soc.* **120**, 2678 (1998).
53. M. L. Mansfield, L. Rakesh, D. A. Tomalia. *J. Chem. Phys.* **105**, 3245 (1996).
54. D. A. Tomalia, S. Uppuluri, D. R. Swanson, H. M. Brothers II, L. T. Piehler, D. J. Meier, G. L. Hagnauer, L. Balogh. In *Mat. Res. Soc. Symp. Proc.*, J. M. Drake, G. S. Grest, J. Klafter, and R. Kopelman (Eds.), Vol. 543, p. 289, Materials Research Society, Boston (1999).
55. S. Uppuluri, L. T. Piehler, J. Li, D. R. Swanson, G. L. Hagnauer, D. A. Tomalia. *Adv. Mater.* **12** (11), 796 (2000).
56. J. Li, D. R. Swanson, D. Qin, H. M. Brothers II, L. T. Piehler, D. A. Tomalia, D. J. Meier. *Langmuir* **15**, 7347 (1999).